

Tetrahedral Imidazolate Frameworks with Auxiliary Ligands

Subjects: Chemistry, Inorganic & Nuclear

Contributor: Tong Hao, Hui-Zi Li, Fei Wang, Jian Zhang

Zeolitic imidazolate frameworks (ZIFs) are an important subclass of metal–organic frameworks (MOFs). A new kind of MOF, namely tetrahedral imidazolate frameworks with auxiliary ligands (TIF-Ax) was reported, by adding linear ligands (Hint) into the zinc–imidazolate system. Introducing linear ligands into the M^{2+} -imidazolate system overcomes the limitation of imidazole derivatives. Thanks to the synergistic effect of two different types of ligands, a series of new TIF-Ax with interesting topologies and a special pore environment has been reported, and they have attracted extensive attention in gas adsorption, separation, catalysis, heavy metal ion capture, and so on.

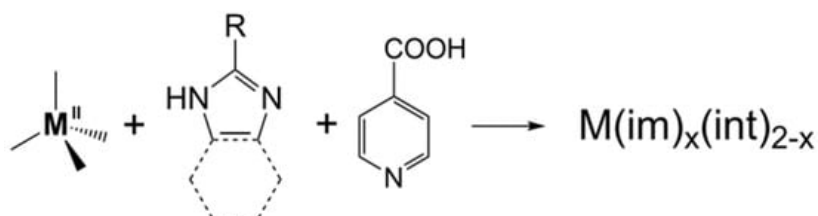
Keywords: zeolite ; metal–organic frameworks ; zeolitic imidazolate frameworks ; tetrahedral imidazolate frameworks ; TIF-A1 ; adsorption and separation

1. Introduction

Zeolite and metal–organic frameworks (MOFs) are two kinds of crystalline porous materials [1][2][3]. Both of them have received much attention not only because of their wide applications but also for their fascinating structures that can be rationally designed and predicted [4][5][6][7]. Recently, zeolitic imidazolate frameworks (ZIFs) have been developed by employing tetrahedral metal ($M^{2+} = Zn^{2+}, Co^{2+}$, etc.) and imidazolate (im^-) derivatives to mimic the tetrahedral center and bridge O in zeolite [8][9][10][11][12][13]. At the same time, the M-im-M (M = metal ion) angle is close to the Si-O-Si angle in zeolite. The network diversity of ZIFs is mainly achieved by changing the substitute groups of imidazole or mixing different imidazolate derivatives (link–link interactions) [3][14][15][16][17][18][19][20][21][22]. ZIFs have been widely used in gas adsorption/separation [23][24][25], catalysis [26][27], electrocatalysis [28][29][30][31][32][33][34][35][36][37], biomedicine [38], and more [39][40][41][42][43][44][45][46]. Considering the wide applications of ZIFs, researchers have never stopped exploring and synthesizing new ZIFs with interesting topologies [47][48].

Theoretically, beyond the limitation of imidazole, any bridge ligand with -1 charge can be used to replace imidazole in ZIFs to construct 4-connected frameworks [49]. In fact, the ZIF analogs based on triazole and tetrazole derivatives and the combination of them have also been reported [11][16][50][51][52][53][54][55][56][57]. Additionally, the attempt of some linear ligands generally leads to the formation of the non-zeolite dia (cubic diamond) topology, suggesting the importance of bent ligands.

In 2011, the researchers reported a new kind of MOF, namely tetrahedral imidazolate frameworks with auxiliary ligands (TIF-Ax), by adding linear ligands into the zinc–imidazolate system (Scheme 1) [22]. The most obvious difference between TIF-Ax and ZIFs is that the introduction of Hint makes the angle of M-int-M larger than that of M-im-M. Therefore, introducing linear ligands into the M^{2+} -imidazolate system overcomes the limitation of imidazole derivatives. Thanks to the synergistic effect of two different types of ligands, a series of new TIF-Ax with interesting topologies and a special pore environment has been reported, and they have attracted extensive attention in gas adsorption, separation, catalysis, heavy metal ion capture, framework flexibility, and so on. More importantly, a variety of facile and rapid synthesis methods have been developed to realize the near-kilogram synthesis of them, paving the way for the large-scale application of TIF-Ax in the future (Table 1).



Scheme 1. Strategy for the synthesis of TIF-Ax.**Table 1.** Summary of reported TIF-Ax.

Name	Formula	Space Group	Topology	Ref.
TIF-A1	$[\text{Zn}(\text{ad})(\text{int})](\text{DMF})$ ¹	<i>Pna2</i> ₁	dmp	[22]
TIF-A2	$\text{Zn}_2(\text{im})_3(\text{int})$ ²	<i>Pca2</i> ₁	dia	[22]
TIF-A3	$\text{Zn}_2(\text{im})(\text{int})_2(\text{OH})$	<i>C2/c</i>	neb	[22]
2-NH ₂ -TIF-A1	$[\text{Zn}(\text{ad})(2\text{-NH}_2\text{-int})](\text{DMF})$	<i>Pna2</i> ₁	dmp	[58]
3-NH ₂ -TIF-A1	$[\text{Zn}(3\text{-NH}_2\text{-int})(\text{ad})](\text{DMF})$ $[\text{Zn}(3\text{-NH}_2\text{-int})(\text{ad})](\text{DMA})$ ³	<i>Pna2</i> ₁	dmp	[59]
Zn-thp-nit	$[\text{Zn}(\text{thp})(\text{nit})]$ ⁴	<i>Pbca</i>	—	[60]
Cd-ad-int	$[\text{Cd}_2(\text{ad})_2(\text{int})_2(\text{DMF})$ $(\text{H}_2\text{O})](\text{DMF})$	<i>P2</i> ₁ / <i>n</i>	mog	[61]
TIF-A4	$\text{Zn}(\text{im})(\text{Ac})$ ⁵	<i>Ima2</i>	dia	[62]
TIF-A5	$\text{Zn}(2\text{-mim})(\text{Ac})$ ⁶	<i>P2</i> ₁ / <i>c</i>	sql	[62]
TIF-A6	$\text{Zn}(2\text{-eim})(\text{Ac})$ ⁷	<i>P2</i> ₁ / <i>c</i>	sql	[62]
TIF-A7	$\text{Zn}(2\text{-pim})(\text{Ac})$ ⁸	<i>Pna2</i> ₁	sql	[62]
TIF-A8	$[\text{Zn}_2(\text{OH})(\text{Ac})(2\text{-cim})_2](\text{DMSO})$ ⁹	<i>Cmc2</i> ₁	sql	[62]

¹ ad = adeninate; int = isonicotinate; DMF = *N,N'*-dimethylformamide; ² im = imidazolate; ³ DMA = *N,N'*-dimethylacetamide; ⁴ thp = theophylline; nit = nicotinic acid; ⁵ Ac = acetic acid; ⁶ mim = 2-methylimidazolate; ⁷ eim = 2-ethylimidazolate; ⁸ pim = 2-propylimidazolate; ⁹ cim = imidazolate-2-carboxaldehyde; DMSO = dimethyl sulfoxide.

2. Synthesis Method

All of the TIF-Ax compounds were initially synthesized using the solvothermal method (for detailed information, refer to the original papers). Based on the solvothermal method, diverse improved methods have been developed to serve various purposes.

2.1. Facile Synthesis

TIF-A1 was originally synthesized by the solvothermal method using $\text{Zn}(\text{NO}_3)_2 \cdot 6\text{H}_2\text{O}$, adenine, and isonicitnic acid (Hint) in *N,N'*-dimethylformamide (DMF) at 120 °C for 3 days with a high yield (88%) [22].

2.2. Metal Sources

Inspired by the aforementioned outcomes achieved through stirring and heating at 120 °C in a brief timeframe, and mindful of the potential for the reaction between nitrate and carboxylic acid to generate corrosive nitric acid, which might compromise the equipment's integrity and influence the stability of the final MOFs, alternative metal sources were

employed to investigate the feasibility of substituting $\text{Zn}(\text{NO}_3)_2 \cdot 6\text{H}_2\text{O}$. Similarly, the yields of TIF-A1 synthesized from ZnO and $\text{Zn}(\text{CH}_3\text{COO})_2 \cdot 2\text{H}_2\text{O}$ were 75.5% and 80.5%, respectively [63]. This shows that the metal source has good substitutability.

2.3. Upscale Synthesis

The potential for synthesizing a kilogram of TIF-A1 was further investigated using the aforementioned methods. Interestingly, through the scaling up of reactant quantities, a yield of over 800 g of TIF-A1 was achieved in a single heating process at 120°C [63]. The resulting samples exhibited a similar crystallinity, morphology, and BET surface area to those obtained through the original solvothermal method.

3. Structure Diversity of TIF-Ax

TIF-A1 is a 4-connected metal-organic framework with Zn^{2+} as the metal center, adenine (ad) as the main ligand, and isonicotinic acid (Hint) as the auxiliary ligand. Both ligands bind to Zn^{2+} via N and carboxyl O on heterocycles. It was observed that TIF-A1~A3 has a different topology, which was regulated by changing the type of imidazole salts in the framework. 2-NH₂-TIF-A1 and 3-NH₂-TIF-A1 were prepared by functional modification, and their functional groups could effectively adjust the pore environment and pore size. Cd-ad-int (int= isonicotinic acid) changed the metal center to have different building units, thus adjusting the structural network. Zn-thp-nit (thp = theophylline, nit = nicotinic acid) changed the isonicotinic acid ligand into nicotinic acid, which changed the angle of connection between the ligand and the metal. In TIF-A4 ~ A8, monocarboxylic acid with a coordination angle of ca. 120° was selected to replace the Hint, and a dia topological structure and layered structure were obtained.

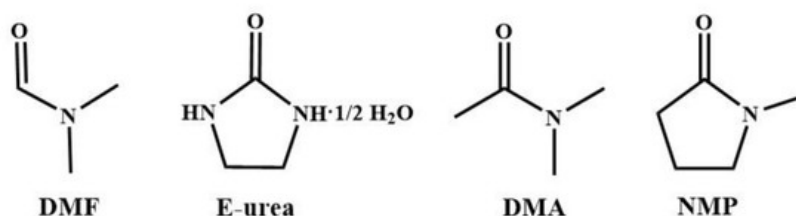
4. Special Properties of TIF-Ax

4.1. Solvent Stability

To realize the wide application of MOFs, they should first have good stability in harsh conditions, such as high temperature, high pressure, and acid and alkali environments. Interestingly, TIF-A1 can be stable in various organic solvents, such as water, *N,N'*-dimethylformamide (DMF), *N,N'*-diethylformamide (DEF), acetonitrile (CH_3CN), ethyl acetate, toluene, *n*-hexane, dichloromethane (DCM), chloroform, methanol (MeOH), ethanol (EtOH), isopropanol (IPA), and *n*-butanol (*n*-BuOH). Furthermore, TIF-A1 can also maintain the framework after being soaked in a solution of pH= 2–1 [63]. The exceptional stability of TIF-A1 makes it a promising candidate for further industrial applications.

4.2. Guest Selectivity

It is well known that solvent plays an important role in the structural variety of MOFs. Different solvent systems tend to produce different MOFs. However, it was found that the construction of TIF-A1 was independent of the solvents. TIF-A1 can accommodate amide solvents, including *N,N'*-dimethylformamide (DMF), ethyl urea (e-urea), *N*-methyl-1,2-pyrrolidone (NMP), and *N,N'*-dimethylacetamide (DMA). Interestingly, the crystallization process of TIF-A1 exhibited a strict selective trapping ability for these four solvent guests, and its selective order was DMF > e-urea > NMP > DMA (Scheme 2). This order of selection may be related to the size of the guest and the interaction between the host and guest. When the size of the guest is relatively small, the size of the guest is the main factor affecting the selection of guest molecules for TIF-A1. The four solvent guests are arranged in that order of molecular size: DMF < DMA < e-urea < NMP. DMF is very suitable to exist in the pores of TIF-A1. When the size of the guest is relatively large, TIF-A1 needs more energy to expand the pore to accommodate them. However, under this condition, the interaction between the host and the guest is dominant, and the energy needed to expand the pore will be partially offset. There is a strong N-H...N hydrogen bond between e-urea and TIF-A1. There are non-classic C-H...O and C-H...N hydrogen bonds between NMP and TIF-A1. There is only a non-classic C-H...O hydrogen bond between DMA and TIF-A1. Therefore, the selection order for TIF-A1 is e-urea > NMP > DMA. However, if the molecule is too large, it still depends mainly on the size of the guest. For example, TIF-A1 cannot trap 1,3-dimethyl-2-imidazolidinone (DMI) or *N,N'*-dimethylpropyleneurea (DMPU) [64].



4.3. Flexibility

As mentioned above, TIF-A1 showed a certain degree of contraction and expansion during crystallization to adapt to different guest molecules. Considering the porosity of TIF-A1, the flexibility of it was further explored by different gases [65]. The de-solvated form denoted as TIF-A1' was obtained through methanol exchange. Unexpectedly, TIF-A1' showed normal adsorption behavior for most common gases, such as N₂, H₂, and CO₂, while it only showed multistep adsorption for C₂H₂. With the combination of in situ single-crystal XRD and calculation simulation, the flexibility of TIF-A1 was derived from the strong interaction between acetylene and the uncoordinated carboxylate O atoms of the int ligand. The C₂H₂-induced flexibility of TIF-A1 is intrinsic and was not affected by the sample size or defects. However, 2-NH₂-TIF-A1 exhibited normal acetylene adsorption because the presence of a strong H-bond between the -NH₂ of ad and the uncoordinated carboxylate O atoms of 2-NH₂-int prevented C₂H₂ from approaching the active site and made the rotation of 2-NH₂-int ligand more complex.

5. Application

5.1. CO₂ Separation

Considering the presence of abundant active sites on TIF-A1, its CO₂ adsorption was first evaluated. After becoming fully activated, TIF-A1 exhibited high CO₂ uptake at 273 K and 1 bar (107 cm³/g) [64]. In contrast, the highest CO₂ adsorption in ZIFs at that time was ZIF-69, with a value of 70 cm³/g [22]. The high CO₂ adsorption capacity of TIF-A1 can be attributed to the synergistic effect of int and ad ligands. Because the -NH₂ group amino and pyrimidine N atoms in ad form an electron-rich system, they are potential CO₂ bond sites. As mentioned above, the uncoordinated carboxylate O atoms of int ligand can also be active sites. In addition, the specific pore size and environment of TIF-A1 also play important roles in CO₂ adsorption. Furthermore, the special interaction between TIF-A1 and CO₂ indicates that TIF-A1 has the potential ability to selectively adsorb CO₂, which makes it possible to apply TIF-A1 in the capture and separation of CO₂ in flue gas. The flue gas mainly contains CO₂ and N₂, which are similar in molecular size, and it is difficult to achieve the separation effect by the pure physical adsorption of porous materials. The N₂ adsorption of TIF-A1 was 4.7 cm³/g (273 K) and 1.4 cm³/g (298 K), which shows that TIF-A1 barely adsorbed N₂. Henry's constant indicates that the adsorption selectivity of TIF-A1 for CO₂ over N₂ was 90 (273 K, 1 bar) and 60 (298 K, 1 bar), respectively [58]. The excellent separation selectivity of TIF-A1 was further demonstrated by a breakthrough experiment [63].

5.2. NH₃ Adsorption

Due to the strong electronegativity of the N sites in TIF-A1, it can not only form an electron-rich system to attract CO₂ but also form a strong hydrogen bond with NH₃. Therefore, the NH₃ adsorption of 3-NH₂-TIF-A1 was studied. At 298 K and 1 bar, the maximum NH₃ adsorption capacities of 3-NH₂-TIF-A1 (obtained in DMA) was 9.8 mmol/g (obtained in DMA) and 7.1 mmol/g (obtained in DMF), which were higher than those of MOF-5 and ultrahigh porous MOF-177 [59]. 3-NH₂-TIF-A1 has abundant active sites, including an uncoordinated oxygen atom and -NH₂ group of 3-NH₂-int, uncoordinated N atoms and -NH₂ group of the ad ligand. Among them, the -NH₂ group on ad and the N of the pyrimidine ring at its para-position had lower E_{ads} values compared to those of the other four sites, which can provide more stable adsorption sites.

5.3. C₂ Separation

In addition to CO₂, TIF-A1 also exhibited a good C₂ separation ability. In 2022, Ding and co-workers applied TIF-A1 to trap C₂H₂ and C₂H₆ simultaneously from the ternary mixture gas of C₂H₂/C₂H₄/C₂H₆ and performed the purification of C₂H₄ [66]. In the ternary mixture of C₂H₂/C₂H₄/C₂H₆, a strong electrostatic interaction occurred between C₂H₂ and the uncoordinated carboxyl O with high polarity in TIF-A1, and van der Waals (vdW) interaction occurred between C₂H₆ and the aromatic heterocycles with low polarity. TIF-A1 not only provides a strong binding site for the adsorption of C₂H₂ and C₂H₆, but also oblate C₂H₆ and linear C₂H₂ are very suitable for the spindle-shaped cage of TIF-A1, which can store the target molecule well. The results show that TIF-A1 separated 99.9% ethylene from C₂H₂/C₂H₄/C₂H₆ (1/10/89) at 298 K and 1 bar, and the yield was 1.43 mmol/g, representing the best purification capacity at that time.

5.4. CO₂ Cycloaddition

In 2021, Wang and co-workers selected ZnX₂ (X = Cl, Br, I) instead of ZnNO₃ and selected a suitable solvent environment to synthesize a series of X-TIF-A1 with many halogen ions in the framework as catalysts for the CO₂ activation reaction [67]. Due to their potent nucleophilic nature, halogen ions induced the ring-opening of propylene oxide, facilitating the

reaction between CO₂ and propylene oxide to generate propylene carbonate—a pivotal step in catalyzing CO₂ conversion. The outcomes demonstrated that the yield of the CO₂ activation reaction catalyzed by ZnI₂-ad-int-DMF exhibited an upward trend with increasing reaction temperature. Notably, the yield achieved an impressive 98.5% at 140 °C. Subsequent to three cycles of reuse, ZnI₂-ad-int-DMF experienced a moderate decline in catalytic activity. However, its framework remained stable despite exposure to high-temperature, high-pressure, and solvent conditions. Importantly, no discernible blocking phenomenon was observed as the iodine content decreased from 69 μmol/g to 51 μmol/g [67].

5.5. Heavy Metal Adsorption

In 2022, Ma and co-workers used chitosan as the TIF-A1 growth template and prepared TIF-A1/chitosan composite beads using a secondary growth method for Pb(II) adsorption in water [68]. Several small TIF-A1 crystals formed rod-shaped clusters and aggregated in the pores of chitosan. The average particle size of TIF-A1/chitosan was 0.2 μm. Such a large composite ball can effectively avoid the harm of pipeline blockage caused by the difficulty of separation and recovery of powdery MOF materials in practical applications. The polar groups -COO⁻, -OH, C=N, and -NH₂ in the TIF-A1/chitosan structure coordinate with Pb(II).

The maximum adsorption of TIF-A1/chitosan for Pb(II) was 397.3 mg/g at 25 °C and pH = 6. Furthermore, in the mixed solution of multiple metal ions, TIF-A1/chitosan hardly adsorbed other ions, and the adsorption removal efficiency of Pb(II) was 99.17%. Especially when the concentration of Pb(II) was 100 ppb, the removal efficiency of trace Pb(II) was 99.95%, and the residual amount of Pb(II) met the international drinking water standards [68]. After five adsorption/desorption cycles, TIF-A1/chitosan could still maintain high adsorption performance, and the removal efficiency was more than 99%. Furthermore, the crystal structure of TIF-A1 was not destroyed, and TIF-A1 was still attached to the chitosan matrix. In conclusion, TIF-A1/chitosan is a promising adsorbent for the removal of trace Pb(II) in drinking water treatment because of its excellent performance and reusability.

References

1. Li, J.; Gao, Z.R.; Lin, Q.-F.; Liu, C.; Gao, F.; Lin, C.; Zhang, S.; Deng, H.; Mayoral, A.; Fan, W.; et al. A 3D extra-large-pore zeolite enabled by 1D-to-3D topotactic condensation of a chain silicate. *Science* 2023, 379, 283–287.
2. Su, Y.; Otake, K.-I.; Zheng, J.-J.; Horike, S.; Kitagawa, S.; Gu, C. Separating water isotopologues using diffusion-regulatory porous materials. *Nature* 2022, 611, 289–294.
3. Tan, Y.-X.; Wang, F.; Zhang, J. Design and synthesis of multifunctional metal–organic zeolites. *Chem. Soc. Rev.* 2018, 47, 2130–2144.
4. Wan, C.P.; Yi, J.D.; Cao, R.; Huang, Y.B. Conductive Metal/Covalent Organic Frameworks for CO₂ Electroreduction. *Chin. J. Struct. Chem.* 2022, 41, 2205001–2205014.
5. Chen, R.; Chen, G.; He, Y.; Zhang, J. Coordination Assembly of Tetrahedral Ti₄(embonate)₆ Cages with Alkaline-Earth Metal Ions. *Chin. J. Struct. Chem.* 2022, 41, 2201001–2201006.
6. Zhang, Y.; Liu, Y.; Wang, D.; Liu, J.; Zhao, J.; Chen, L. State-of-the-art advances in the syntheses, structures, and applications of polyoxometalate-based metal–organic frameworks. *Polyoxometalates* 2023, 2, 9140017.
7. Dao, X.-Y.; Sun, W.-Y. Single- and mixed-metal-organic framework photocatalysts for carbon dioxide reduction. *Inorg. Chem. Front.* 2021, 8, 3178–3204.
8. Huang, X.-C.; Lin, Y.-Y.; Zhang, J.-P.; Chen, X.-M. Ligand-Directed Strategy for Zeolite-Type Metal–Organic Frameworks: Zinc(II) Imidazoles with Unusual Zeolitic Topologies. *Angew. Chem. Int. Ed.* 2006, 45, 1557–1559.
9. Banerjee, R.; Phan, A.; Wang, B.; Knobler, C.; Furukawa, H.; O’Keeffe, M.; Yaghi, O.M. High-Throughput Synthesis of Zeolitic Imidazolate Frameworks and Application to CO₂ Capture. *Science* 2008, 319, 939–943.
10. Tian, Y.-Q.; Yao, S.-Y.; Gu, D.; Cui, K.-H.; Guo, D.-W.; Zhang, G.; Chen, Z.-X.; Zhao, D.-Y. Cadmium Imidazolate Frameworks with Polymorphism, High Thermal Stability, and a Large Surface Area. *Chem.-A Eur. J.* 2010, 16, 1137–1141.
11. Zhang, J.-P.; Zhu, A.-X.; Lin, R.-B.; Qi, X.-L.; Chen, X.-M. Pore Surface Tailored SOD-Type Metal–Organic Zeolites. *Adv. Mater.* 2011, 23, 1268–1271.
12. He, C.-T.; Jiang, L.; Ye, Z.-M.; Krishna, R.; Zhong, Z.-S.; Liao, P.-Q.; Xu, J.; Ouyang, G.; Zhang, J.-P.; Chen, X.-M. Exceptional Hydrophobicity of a Large-Pore Metal–Organic Zeolite. *J. Am. Chem. Soc.* 2015, 137, 7217–7223.
13. Xu, T.; Zhou, B.; Tao, Y.; Shi, Z.; Jiang, W.; Abdellatif, M.; Cordova, K.E.; Zhang, Y.-B. Functionality-Induced Locking of Zeolitic Imidazolate Frameworks. *Chem. Mater.* 2023, 35, 490–498.

14. Yang, J.; Zhang, Y.-B.; Liu, Q.; Trickett, C.A.; Gutiérrez-Puebla, E.; Monge, M.Á.; Cong, H.; Aldossary, A.; Deng, H.; Yaghi, O.M. Principles of Designing Extra-Large Pore Openings and Cages in Zeolitic Imidazolate Frameworks. *J. Am. Chem. Soc.* 2017, 139, 6448–6455.
15. Eddaoudi, M.; Sava, D.F.; Eubank, J.F.; Adil, K.; Guillerm, V. Zeolite-like metal–organic frameworks (ZMOFs): Design, synthesis, and properties. *Chem. Soc. Rev.* 2015, 44, 228–249.
16. Li, M.-Y.; Liu, J.; Gao, R.; Lin, D.-Y.; Wang, F.; Zhang, J. Design and synthesis of zeolitic tetrazolate-imidazolate frameworks. *Mater. Today Adv.* 2021, 10, 100145.
17. Zhang, J.-P.; Zhang, Y.-B.; Lin, J.-B.; Chen, X.-M. Metal Azolate Frameworks: From Crystal Engineering to Functional Materials. *Chem. Rev.* 2012, 112, 1001–1033.
18. Wu, T.; Bu, X.; Zhang, J.; Feng, P. New Zeolitic Imidazolate Frameworks: From Unprecedented Assembly of Cubic Clusters to Ordered Cooperative Organization of Complementary Ligands. *Chem. Mater.* 2008, 20, 7377–7382.
19. Wu, T.; Bu, X.; Liu, R.; Lin, Z.; Zhang, J.; Feng, P. A New Zeolitic Topology with Sixteen-Membered Ring and Multidimensional Large Pore Channels. *Chem.-A Eur. J.* 2008, 14, 7771–7773.
20. Zheng, S.-T.; Li, Y.; Wu, T.; Nieto, R.A.; Feng, P.; Bu, X. Porous Lithium Imidazolate Frameworks Constructed with Charge-Complementary Ligands. *Chem.-A Eur. J.* 2010, 16, 13035–13040.
21. Zheng, S.; Wu, T.; Zhang, J.; Chow, M.; Nieto, R.A.; Feng, P.; Bu, X. Porous Metal Carboxylate Boron Imidazolate Frameworks. *Angew. Chem. Int. Ed.* 2010, 49, 5362–5366.
22. Wang, F.; Tan, Y.-X.; Yang, H.; Zhang, H.-X.; Kang, Y.; Zhang, J. A new approach towards tetrahedral imidazolate frameworks for high and selective CO₂ uptake. *Chem. Commun.* 2011, 47, 5828–5830.
23. Peng, Y.; Li, Y.; Ban, Y.; Jin, H.; Jiao, W.; Liu, X.; Yang, W. Metal-organic framework nanosheets as building blocks for molecular sieving membranes. *Science* 2014, 346, 1356–1359.
24. Abdul Hamid, M.R.; Shean Yaw, T.C.; Mohd Tohir, M.Z.; Wan Abdul Karim Ghani, W.A.; Sutrisna, P.D.; Jeong, H.-K. Zeolitic imidazolate framework membranes for gas separations: Current state-of-the-art, challenges, and opportunities. *J. Ind. Eng. Chem.* 2021, 98, 17–41.
25. Guan, W.; Dai, Y.; Dong, C.; Yang, X.; Xi, Y. Zeolite imidazolate framework (ZIF)-based mixed matrix membranes for CO₂ separation: A review. *J. Appl. Polym. Sci.* 2020, 137, 48968.
26. Zanon, A.; Verpoort, F. Metals@ZIFs: Catalytic applications and size selective catalysis. *Coord. Chem. Rev.* 2017, 353, 201–222.
27. Williams, K.; Meng, L.; Lee, S.; Lux, L.; Gao, W.; Ma, S. Imparting brønsted acidity into a zeolitic imidazole framework. *Inorg. Chem. Front.* 2016, 3, 393–396.
28. Gao, C.; Mu, S.; Yan, R.; Chen, F.; Ma, T.; Cao, S.; Li, S.; Ma, L.; Wang, Y.; Cheng, C. Recent Advances in ZIF-Derived Atomic Metal–N–C Electrocatalysts for Oxygen Reduction Reaction: Synthetic Strategies, Active Centers, and Stabilities. *Small* 2022, 18, 2105409.
29. Ahmad, R.; Khan, U.A.; Iqbal, N.; Noor, T. Zeolitic imidazolate framework (ZIF)-derived porous carbon materials for supercapacitors: An overview. *RSC Adv.* 2020, 10, 43733–43750.
30. Arafat, Y.; Azhar, M.R.; Zhong, Y.; Abid, H.R.; Tadé, M.O.; Shao, Z. Advances in Zeolite Imidazolate Frameworks (ZIFs) Derived Bifunctional Oxygen Electrocatalysts and Their Application in Zinc–Air Batteries. *Adv. Energy Mater.* 2021, 11, 2100514.
31. Song, X.; Jiang, Y.; Cheng, F.; Earnshaw, J.; Na, J.; Li, X.; Yamauchi, Y. Hollow Carbon-Based Nanoarchitectures Based on ZIF: Inward/Outward Contraction Mechanism and Beyond. *Small* 2021, 17, 2004142.
32. Dutta, S.; Liu, Z.; Han, H.; Indra, A.; Song, T. Electrochemical Energy Conversion and Storage with Zeolitic Imidazolate Framework Derived Materials: A Perspective. *ChemElectroChem* 2018, 5, 3571–3588.
33. Cheng, N.; Ren, L.; Xu, X.; Du, Y.; Dou, S.X. Recent Development of Zeolitic Imidazolate Frameworks (ZIFs) Derived Porous Carbon Based Materials as Electrocatalysts. *Adv. Energy Mater.* 2018, 8, 1801257.
34. Yang, H.; Chen, X.; Chen, W.-T.; Wang, Q.; Cuello, N.C.; Nafady, A.; Al-Enizi, A.M.; Waterhouse, G.I.N.; Goenaga, G.A.; Zawodzinski, T.A.; et al. Tunable Synthesis of Hollow Metal–Nitrogen–Carbon Capsules for Efficient Oxygen Reduction Catalysis in Proton Exchange Membrane Fuel Cells. *ACS Nano* 2019, 13, 8087–8098.
35. Hou, C.-C.; Xu, Q. Metal–Organic Frameworks for Energy. *Adv. Energy Mater.* 2019, 9, 1801307.
36. Wang, H.-F.; Chen, L.; Pang, H.; Kaskel, S.; Xu, Q. MOF-derived electrocatalysts for oxygen reduction, oxygen evolution and hydrogen evolution reactions. *Chem. Soc. Rev.* 2020, 49, 1414–1448.

37. Yang, Q.; Xu, Q.; Yu, S.-H.; Jiang, H.-L. Pd Nanocubes@ZIF-8: Integration of Plasmon-Driven Photothermal Conversion with a Metal–Organic Framework for Efficient and Selective Catalysis. *Angew. Chem. Int. Ed.* 2016, 55, 3685–3689.
38. Maleki, A.; Shahbazi, M.-A.; Alinezhad, V.; Santos, H.A. The Progress and Prospect of Zeolitic Imidazolate Frameworks in Cancer Therapy, Antibacterial Activity, and Biomineralization. *Adv. Healthc. Mater.* 2020, 9, 2000248.
39. Zhao, Z.; Gao, Z.; Lan, D.; Kou, K. MOFs-derived hollow materials for electromagnetic wave absorption: Prospects and challenges. *J. Mater. Sci. Mater. Electron.* 2021, 32, 25631–25648.
40. Hou, J.; Ashling, C.W.; Collins, S.M.; Krajnc, A.; Zhou, C.; Longley, L.; Johnstone, D.N.; Chater, P.A.; Li, S.; Coulet, M.-V.; et al. Metal-organic framework crystal-glass composites. *Nat. Commun.* 2019, 10, 2580.
41. Madsen, R.S.K.; Qiao, A.; Sen, J.; Hung, I.; Chen, K.; Gan, Z.; Sen, S.; Yue, Y. Ultrahigh-field ^{67}Zn NMR reveals short-range disorder in zeolitic imidazolate framework glasses. *Science* 2020, 367, 1473–1476.
42. Ma, N.; Horike, S. Metal–Organic Network-Forming Glasses. *Chem. Rev.* 2022, 122, 4163–4203.
43. Fonseca, J.; Gong, T.; Jiao, L.; Jiang, H.-L. Metal–organic frameworks (MOFs) beyond crystallinity: Amorphous MOFs, MOF liquids and MOF glasses. *J. Mater. Chem. A* 2021, 9, 10562–10611.
44. Cai, G.; Yan, P.; Zhang, L.; Zhou, H.-C.; Jiang, H.-L. Metal–Organic Framework-Based Hierarchically Porous Materials: Synthesis and Applications. *Chem. Rev.* 2021, 121, 12278–12326.
45. Gao, S.; Hou, J.; Deng, Z.; Wang, T.; Beyer, S.; Buzanich, A.G.; Richardson, J.J.; Rawal, A.; Seidel, R.; Zulkifli, M.Y.; et al. Improving the Acidic Stability of Zeolitic Imidazolate Frameworks by Biofunctional Molecules. *Chem* 2019, 5, 1597–1608.
46. Yang, X.-G.; Zhang, J.-R.; Tian, X.-K.; Qin, J.-H.; Zhang, X.-Y.; Ma, L.-F. Enhanced Activity of Enzyme Immobilized on Hydrophobic ZIF-8 Modified by Ni^{2+} Ions. *Angew. Chem.-Int. Ed.* 2023, 62, e202216699.
47. Guo, S.; Li, H.-Z.; Wang, Z.-W.; Zhu, Z.-Y.; Zhang, S.-H.; Wang, F.; Zhang, J. Syntheses of new zeolitic imidazolate frameworks in dimethyl sulfoxide. *Inorg. Chem. Front.* 2022, 9, 2011–2015.
48. Wang, H.; Pei, X.; Kalmutzki, M.J.; Yang, J.; Yaghi, O.M. Large Cages of Zeolitic Imidazolate Frameworks. *Acc. Chem. Res.* 2022, 55, 707–721.
49. Li, M.Y.; Wang, F.; Gu, Z.G.; Zhang, J. Synthesis of homochiral zeolitic metal-organic frameworks with amino acid and tetrazolates for chiral recognition. *RSC Adv.* 2017, 7, 4872–4875.
50. Wang, F.; Hou, D.-C.; Yang, H.; Kang, Y.; Zhang, J. Tetrahedral tetrazolate frameworks for high CO_2 and H_2 uptake. *Dalton Trans.* 2014, 43, 3210–3214.
51. Wang, F.; Fu, H.-R.; Kang, Y.; Zhang, J. A new approach towards zeolitic tetrazolate-imidazolate frameworks (ZTIFs) with uncoordinated N-heteroatom sites for high CO_2 uptake. *Chem. Commun.* 2014, 50, 12065–12068.
52. Zha, X.; Li, X.; Al-Omari, A.A.; Liu, S.; Liang, C.-C.; Al-Ghourani, A.A.; Abdellatif, M.; Yang, J.; Nguyen, H.L.; Al-Maythaly, B.; et al. Zeolite NPO-Type Azolate Frameworks. *Angew. Chem. Int. Ed.* 2022, 61, e202207467.
53. Gai, Y.; Chen, X.; Yang, H.; Wang, Y.; Bu, X.; Feng, P. A new strategy for constructing a disulfide-functionalized ZIF-8 analogue using structure-directing ligand-ligand covalent interaction. *Chem. Commun.* 2018, 54, 12109–12112.
54. Cui, P.; Ma, Y.G.; Li, H.H.; Zhao, B.; Li, J.R.; Cheng, P.; Balbuena, P.B.; Zhou, H.C. Multipoint interactions enhanced CO_2 uptake: A zeolite-like zinc-tetrazole framework with 24-nuclear zinc cages. *J. Am. Chem. Soc.* 2012, 134, 18892–18895.
55. Qin, J.S.; Du, D.Y.; Li, W.L.; Zhang, J.P.; Li, S.L.; Su, Z.M.; Wang, X.L.; Xu, Q.; Shao, K.Z.; Lan, Y.Q. N-rich zeolite-like metal-organic framework with sodalite topology: High CO_2 uptake, selective gas adsorption and efficient drug delivery. *Chem. Sci.* 2012, 3, 2114–2118.
56. Tang, Y.H.; Wang, F.; Liu, J.X.; Zhang, J. Diverse tetrahedral tetrazolate frameworks with N-rich surface. *Chem. Commun.* 2016, 52, 5625–5628.
57. Wang, F.; Tang, Y.H.; Zhang, J. Achievement of Bulky Homochirality in Zeolitic Imidazolate-Related Frameworks. *Inorg. Chem.* 2015, 54, 11064–11066.
58. Yang, E.; Li, H.-Y.; Wang, F.; Yang, H.; Zhang, J. Enhancing CO_2 adsorption enthalpy and selectivity via amino functionalization of a tetrahedral framework material. *CrystEngComm* 2013, 15, 658–661.
59. Ruan, M.; Li, A.; Wen, Y.; Zhou, L.; Zhang, J.; Xuan, X. Adenine-based bio-MOFs with high water and acid–base stability for ammonia capture. *CrystEngComm* 2022, 24, 7420–7426.
60. Lou, B.; He, F. Coordination polymers as potential solid forms of drugs: Three zinc(ii) coordination polymers of theophylline with biocompatible organic acids. *New J. Chem.* 2013, 37, 309–316.

61. Wang, F.; Kang, Y. Unusual cadmium(II)–adenine paddle-wheel units for the construction of a metal-organic framework with mog topology. *Inorg. Chem. Commun.* 2012, 20, 266–268.
62. Guo, S.; Zhang, S.-H.; Wang, F.; Zhang, J. Syntheses of tetrahedral imidazolate frameworks with auxiliary ligand in DMSO. *J. Solid State Chem.* 2022, 311, 123101.
63. Li, H.-Z.; Sun, Y.; Lin, D.; Yang, W.; Wang, F. Facile syntheses of tetrahedral imidazolate framework for CO₂ separation. *J. Solid State Chem.* 2021, 297, 122100.
64. Wang, F.; Yang, H.; Kang, Y.; Zhang, J. Guest selectivity of a porous tetrahedral imidazolate framework material during self-assembly. *J. Mater. Chem.* 2012, 22, 19732–19737.
65. Li, H.-Z.; Li, Q.-H.; Yao, M.; Han, Y.-P.; Otake, K.-I.; Kitagawa, S.; Wang, F.; Zhang, J. Metal–Organic Framework with Structural Flexibility Responding Specifically to Acetylene and Its Adsorption Behavior. *ACS Appl. Mater. Interfaces* 2022, 14, 45451–45457.
66. Ding, Q.; Zhang, Z.; Liu, Y.; Chai, K.; Krishna, R.; Zhang, S. One-Step Ethylene Purification from Ternary Mixtures in a Metal–Organic Framework with Customized Pore Chemistry and Shape. *Angew. Chem. Int. Ed.* 2022, 61, e202208134.
67. Wang, J.-X.; Li, H.-G.; Ye, S.-S.; Zhang, J.-B.; Chen, B.-H. Halogen-rich zinc-adeninate framework construction and its catalytic performance on CO₂ cycloaddition without cocatalyst. *CIESC J.* 2021, 72, 3686–3695.
68. Ma, Y.; You, D.; Fang, Y.; Luo, J.; Pan, Q.; Liu, Y.; Wang, F.; Yang, W. Confined growth of MOF in chitosan matrix for removal of trace Pb(II) from reclaimed water. *Sep. Purif. Technol.* 2022, 294, 121223.

Retrieved from <https://encyclopedia.pub/entry/history/show/110568>